University of Bath

Alternative formats
If you require this document in an alternative format, please contact:
openaccess@bath.ac.uk

Enhanced colorimetric differentiation between *Staphylococcus aureus* and *Pseudomonas aeruginosa* using a shape-encoded sensor hydrogel

Zhiyuan Jia[a], Lauren Gwynne[b], Adam C. Sedgwick[c], Mareike Müller[a], George T. Williams[b], Andrew Toby A. Jenkins[b], Tony James[b], Holger Schönherr[a]*

[a] Physical Chemistry I & Research Center of Micro and Nanochemistry and Engineering (*Cµ*), Department of Chemistry and Biology, University of Siegen, Adolf-Reichwein-Straße 2, 57076 Siegen, Germany

[b] Department of Chemistry, University of Bath, Bath, BA2 7AY, UK

[c] Department of Chemistry, The University of Texas at Austin, 105 E 24th street A5300, Austin, TX 78712-1224 (USA)

* corresponding author: schoenherr@chemie.uni-siegen.de

ABSTRACT

Herein, we demonstrate a combined fluorescent probe/shape encoded hydrogel strategy for the fast, sensitive and selective detection of bacterial species via their characteristic enzymes. A polyvinyl alcohol (PVA) hydrogel loaded with the fluorescent probe *N,N'*-(3-oxo-3H-spiro[isobenzofuran-1,9'-xanthene]-3',6'-diyl)bis(2,2,3,3,3-pentafluoropropanamide) (**ACS-HNE**) was designed for the detection of elastase, an enzyme produced by *Pseudomonas aeruginosa*. Likewise, a chitosan-derived hydrogel was loaded with the fluorescent probe 4-methylumbelliferyl-α-D-glucopyranoside (**MUD**) by entrapment for the selective detection of α-glucosidase, an enzyme produced by *Staphylococcus aureus*. For an observation time of 60 minutes, limits of detection (LOD) of ≤ 20 nM for elastase and ≤ 30 pM for α-glucosidase were obtained, which in the latter case is three orders of magnitude better than related chitosan systems with covalently coupled substrate. To illustrate the potential utility of these highly sensitive sensor hydrogels as a simple point-of-care test system, shaped hydrogel slabs representing the letters **P** and **S** were manufactured to detect *Pseudomonas aeruginosa* and *Staphylococcus aureus,* respectively. These shapes were shown to provide an additional unique color code under UV illumination corresponding to the characteristic enzyme produced by the corresponding bacteria. This study shows potential for the future development of an effective and simple point-of-care test for the rapid identification of bacterial species that can be operated by non-specialists.

INTRODUCTION

Pseudomonas aeruginosa (*P. aeruginosa*) and *Staphylococcus aureu*s (*S. aureus*) are two clinically relevant multi-drug resistant (MDR) pathogenic bacteria that pose a significant threat to public health due to the lack of therapeutic alternatives.[1] *P. aeruginosa* is responsible for a variety of healthcare-associated infections, including pneumonia, bloodstream infections, urinary tract infections, and surgical site infections, and is particularly dangerous for immunocompromised patients.[2] In the United States alone, 51,000 healthcare-associated *P. aeruginosa* infections have been documented, with roughly 400 deaths each year attributed to MDR *P. aeruginosa*.[3] *S. aureus* is a leading cause of bacteremia and infective endocarditis, as well as osteoarticular, skin and soft tissue, pleuropulmonary, and device-related infections and food poisoning.[4,5,6] Methicillin-resistant *S. aureus* (MRSA) is resistant to numerous antibiotics, and as such causes life-threatening bloodstream infections, pneumonia, and surgical site infections.[7] Nearly 20,000 deaths were caused by infections with *S. aureus* in 2017 in the United States.[8]

The alarming increase in reports on antibiotic resistance clearly highlights the urgent need for the development of new and effective therapeutics capable of treating such infections. Similarly, new diagnostic platforms capable of rapidly and selectively detecting pathogens are in increasing demand to limit the use of antibiotics and offer a targeted treatment tailored to the needs of affected patients.

To date, the most common methods for bacterial detection involve direct or indirect counting of bacteria, molecular diagnostic techniques (i.e. polymerase chain reaction, PCR) and immunology-based assays. The latter approaches are based on DNA analysis and antigen–antibody interactions, respectively.[9,10,11] While they offer high sensitivity, these methods are

time-consuming and require qualified personnel and specialized equipment. Additionally, certain methods, such as indirect counting and PCR, cannot discriminate between viable and non-viable cells.[12,13,14]

Recently, fast, sensitive, selective and reliable bacterial detection methods have been developed based on dedicated laboratory-based equipment or by combining existing methods. These approaches include PCR-enzyme-linked immunosorbent assays,[15] secondary electrospray ionization tandem or matrix assisted laser desorption/ionization-time of flight mass spectrometry,[16,17] and confocal laser scanning microscopy equipped with white light laser technology.[18] However, these newer approaches are usually complicated, expensive, require training of personnel, and are therefore not suitable for application in non-laboratory settings.

Hence the development of point-of-care diagnostic devices, which are cost-effective, accurate, rapid and easy-to-use, also for application in remote areas without appropriate electricity or climate control, etc., has received considerable attention. For instance, Suaifan *et al.* reported a paper-based biosensor, which is able to produce a signal within one minute and which possesses corresponding limits of detection (LOD) as low as 7, 40, and 100 CFU/mL for pure broth cultures of *S. aureus*, *S. aureus* inoculated in food matrices and *S. aureus* in environmental samples, respectively.[19] In this approach, magnetic nanobeads carrying a *S. aureus* protease specific peptide substrate were attached on a gold sensor platform. A visible color change was observed after dissociation of the magnetic nanobead moieties due to the proteolytic activity of *S. aureus* proteases on the specific peptide substrate. In related work, Xu and co-workers developed a sensitive multiple loop-mediated isothermal amplification and lateral flow nucleic acid biosensor to sense *P. aeruginosa* with a LOD as low as 20 CFU/mL. The results could be read out by bare eye within 50 min.[20]

Hydrogels, due to their specific functionality, have also been used for the detection of bacteria and bacterial infections.[21,22] For example, Mirani et al. reported a multifunctional pH sensitive hydrogel-based dressing for the detection of *P. aeruginosa* and *S. aureus* infections via color changes, caused by the pH change after pathogenic infection. The dressing also released drugs at the wound site.[23]

As an alternative colorimetric approach, we have recently reported on autonomously sensing chitosan hydrogels equipped with covalently coupled chromogenic substrates, such as *N*-succinyl-tri-L-alanine 4-nitroanilide and the fluorescent probe 4-methylumbelliferyl α-D-glucopyranoside (MUD), to detect and differentiate neat bacterial enzymes (elastase and α-glucosidase). This approach also worked with supernatants collected from *P. aeruginosa* (PAO1) and *S. aureus* (AGR+, AGR-).[24] The LOD values for an observation time of 1 hour were <45 nM for elastase and <20 nM for α-glucosidase.[24] In all these cases, bacterial enzymes were utilized as a detection target for diagnostic platforms.

Most clinical *P. aeruginosa* strains produce elastase, which is a major virulence factor in *P. aeruginosa*. As metallopeptidase the enzyme hydrolyzes elastin and thus causes immense damage to the connective tissue during the pathogenesis of infections.[25,26,27] Meanwhile, *S. aureus* strains produce α-glucosidase, an exoglycosidase, which hydrolyses terminal, non-reducing (1->4)-linked α-D-glucose residues resulting in the release of α-D-glucose.[24]

The improvement of the sensitivity of these autonomous reporting hydrogels can be pursued by developing novel fluorescent probes and by optimizing the hydrogel properties. For instance, novel fluorescent probes showed excellent performance in staining, classification or differentiation of bacteria species.[28,29,30,31] The bacteria Gram-positive orange (BacGO) fluorescent probe was successfully applied for the detection of low numbers of bacteria of *S.*

aureus among *P. aeruginosa in vivo* due to its selectivity and high sensitivity for Gram-positive bacteria.[32] Additionally, the phosphorylated fluorescent probe 2-hydroxychalcone (HCAP) was utilized in both aqueous and solid phase (by conjugation of the fluorescent probe with an adhesive cationic polymer) for the detection of *Escherichia coli* and *S. aureus*.[33]

In this work reported here, we focused on the improvement of the LOD of hydrogel-based colorimetric reporter systems, and the implementation of an easy readout for the rapid detection and differentiation of *P. aeruginosa* and *S. aureus* also in cultures via both color and shape. The novel rhodamine-based fluorescent probe **ACS-HNE**[34] and the known probe MUD**,** which allow for selective detection of elastase and α-glucosidase, respectively, were loaded by entrapment into optimized hydrogel matrices. The performance of the hydrogels was systematically studied *in vitro* and a simple point-of-care test system, manufactured as shaped hydrogel slabs representing the letters P and S, which code for *Pseudomonas aeruginosa* and *Staphylococcus aureus,* respectively, was developed and successfully tested with bacterial cultures.

EXPERIMENTAL

Materials. Silicon (100) wafers (P/Boron type, manufactured by OKMETIC, Finland), transparent plastic films (Kopier-Folien CE 6088, Germany) and TC Plate 96 Well (transparent and black, Sarstedt, Germany) were used as supporting substrates. Polydimethylsiloxane (PDMS) prepolymer and curing agent (Sylgard 184) were purchased from Dow Corning. Chitosan (medium molar mass, 190−310 kDa, 75−85% deacetylated), succinic anhydride, phosphate-buffered saline (PBS, tablet), α-glucosidase from *Saccharomyces cerevisiae* (16.13 units/mg protein, E.C. 3.2.1.20; type I), Elastase from porcine pancreas (7 units/mg, E.C. 3.4.21.36), dimethyl sulfoxide (DMSO, 99%), Poly(vinyl alcohol) (M_w = 89,000 - 98,000 g/mol)

were purchased from Sigma-Aldrich. Acetone (99%, VWR), Sodium hydroxide (98.8%, Chemsolute), 4-Methylumbelliferyl α-D-glucopyranoside (MUD, Roth) were purchased from listed suppliers. Milli-Q water obtained from Millipore Direct Q 8 system (Millipore, Schwalbach, Germany) with a resistivity of 18 MΩ cm was used for preparation of all aqueous media.

Fluorescence spectroscopy. Measurements were carried out either with a Varian Cary Eclipse spectrometer (Mulgrave, Victoria, Australia) or with microplate readers (Tecan SAFIRE, Tecan, Switzerland; SPECTROstar Omega, BMG LABTECH, Germany) at 25°C. Fluorescence spectra obtained with the Varian Cary Eclipse spectrometer were measured at a scan rate of 120 nm/minute and a resolution of 5 nm for the excitation and emission, using a 1 mm path-length quartz cell (SUPRASIL, Hellma Analytics, Germany). Using the microplate reader fluorescence intensities were recorded using 96 well plates (black, polystyrene, flat bottom, Sarstedt, Germany) as sample holder with a sealing film (Greiner Bio-One, Austria). A bandwidth of 12 nm was applied for both excitation and emission. The gain parameter was manually set to 70 for the Tecan SAFIRE.

Preparation of fluorescent probe loaded hydrogel.

Synthesis of N-succinyl-chitosan (NSC). NSC was prepared by ring-opening reaction using succinic anhydride in DMSO) according to literature.[35,36] Briefly, chitosan (2.0 g) was added to 40 mL DMSO containing succinic anhydride (2.0 g) and stirred for 24 hours at 60 °C. The resultant mixture was filtered (Whatman no. 5 qualitative filter paper), and the obtained solid was washed with alternative rounds of ethanol and acetate before further filtration. Afterwards, the precipitate was dispersed into 100 mL Milli-Q water. A clear suspension was obtained via adjusting the pH to 10-12 by using NaOH solution (1 M). The solution was filtered twice, and

the filtrate was re-precipitated in acetone. The final product was washed with ethanol and acetone and dried under vacuum at 50°C.

Preparation of MUD loaded NSC hydrogels. Aqueous NSC (1.4% (w/v), PBS pH 7.4) was mixed with MUD (0.2, 1.0, 2.0, 5.0mM, $V_{(DMSO)}$: $V_{(PBS)}$=1:49) and deposited into 96 well plates ($V_{(NSC)}$: $V_{(MUD)}$ = 1, 100 µL, black). NSC hydrogels with various MUD loading were applied for the determination of values of the LOD. For hydrogels supported in silicon wafers, 108 µL of a solution containing equal volumes of aqueous NSC solution (4.2% (w/v), PBS pH 7.4) and MUD solution (2 mM, $V_{(DMSO)}$: $V_{(PBS)}$=1:49) was deposited on a cleaned silicon wafer (wafer size: 0.9 × 1.2 cm^2). Hydrogel layers were formed after drying in a clean hood for 24 hours.

*Preparation of **ACS-HNE** loaded PVA hydrogels.* Aqueous PVA solution (20% (w/v)) mixed with **ACS-HNE** solution (10 µM, $V_{(DMSO)}$: $V_{(PBS)}$=1:49) was deposited into 96 well plates ($V_{(PVA)}$: $V_{(ACS-HNE)}$ = 1:100 µL, black) or on a cleaned silicon wafer (*$V_{(PVA)}$:* $V_{(ACS-HNE)}$ = 1:108 µL, wafer size: 0.9 × 1.2 cm^2). Hydrogel layers were formed after drying in a clean hood for 24 hours.

Preparation of patterned samples

PDMS mask preparation. The PDMS mask was prepared according to literature.[37] The PDMS prepolymer and curing agent (Sylgard 184) were mixed in a 10:1 ratio (by weight). After degassing for 30 min, the clear solution was poured into a polystyrene petri dish and cured for 1 hour in an oven at 70°C. After cooling to ambient temperature, cured PDMS was chiseled to form P- and S-shaped holes (16 mm in length and 2.8 mm in thickness).

Preparation of patterned hydrogels loaded with fluorescent probe. Four of each P and S-shaped PDMS masks were attached on a cleaned transparent plastic film (2.6 × 7.6 cm^2, Kopier-Folien CE 6088, Germany) into two columns. Aqueous PVA solution (20% (*w/V*)) mixed with **ACS-HNE** (10 µM, $V_{(DMSO)}$: $V_{(PBS)}$=1:49) was deposited into each P-shaped hole ($V_{(PVA)}$: $V_{(ACS-HNE)}$ =

1, 100 µL) and aqueous NSC solution (1.4% (w/v), PBS, pH 7.4) mixed with MUD (2 mM, $V_{(DMSO)}$: $V_{(PBS)}$=1:49) was deposited into each S-shaped hole ($V_{(NSC)}$: $V_{(MUD)}$=1, 100 µL). Hydrogel layers were formed after drying in a clean hood for 24 hours.

Enzymatic Reactions.

Enzymatic reactions in the hydrogels in 96 well plates.

Varying concentrations of elastase and α-glucosidase (100 µL, PBS, pH 7.4) were added to wells containing their corresponding fluorescent probe-loaded hydrogels. The plate was immediately covered with a sealing film and the fluorescence intensity was measured in a microplate reader. The details of the measurement parameters are mentioned in the captures of corresponding Figures.

Enzymatic reactions in the hydrogels on silicon substrate. An elastase or α-glucosidase sensing hydrogel formed on a silicon substrate was inserted into 1 mm path-length quartz cell. The quartz cell was closed with Parafilm after the addition of buffered elastase (10 µM, 150 µL, PBS, pH 7.4) or α-glucosidase (1 µM, 150 µL, PBS, pH 7.4) enzyme solution. The fluorescence spectra were recorded via a spectrometer immediately. The details of the measurement parameter are mentioned in the captions of corresponding results (Figure 2a and 4a).

Enzymatic reactions in the patterned hydrogels. To both elastase and α-glucosidase sensing hydrogels in 96-well plates, individual buffered enzyme solutions (PBS, pH 7.4) of α-glucosidase (1 µM, 80 µL) or elastase (10 µM, 80 µL) were added into each well of the 1st or 2nd row of the 96-well plate, respectively. 80 µL of a mixture of buffered enzyme solution (40 µL each of α-glucosidase solution, 2 µM, and elastase solution, 20 µM) was dropped in each well in the 3rd row. As the blank, PBS was added into each well in the 4th row. The color change in the patterned areas were recorded during the enzymatic reaction with an iSight camera (iPhone 5s)

under UV illumination with a hand-held standard UV lamp (λ = 365 nm) in front of a black background.

Determination of the Limit of Detection (LOD).

Varying concentrations of α-glucosidase and elastase and (100 µL, PBS, pH 7.4) were added to wells containing their corresponding fluorescent probe-loaded hydrogels. The kinetics of the enzymatic reactions was recorded at a fixed wavelength of 365 nm for α-glucosidase-sensing hydrogels and 496 nm for elastase-sensing hydrogels. The baseline was recorded from a control well, which contained the fluorescent probe-loaded hydrogel and 100 µL of PBS solution.

To determine the LOD for the enzymes, the kinetics of the α-glucosidase/elastase-catalyzed reaction were recorded by sequential I_F measurements at λ_{max} = 450 nm (α-glucosidase-sensing hydrogel) or λ_{max} =527 nm (elastase-sensing hydrogel) using λ_{ex} = 365 nm (α-glucosidase-sensing hydrogel) or λ_{ex} = 496 nm (elastase-sensing hydrogel), respectively. The initial apparent reaction rate was defined as the slope in the first 10 minutes (α-glucosidase-sensing hydrogel) or 30 minutes (elastase-sensing hydrogel) in the kinetics plot and was obtained from a linear least squares fit. As reported in previously published work,[34, 38] the LODs for the liberated 4-methylumbelliferone (4-MU) and rhodamine 110 (RH 110) are 0.1 µmol/L and 1.7 nmol/L, and the value of the lowest detectable signal for microplate reader at 25°C were equal to 21 a.u. and 19 a.u., respectively. Hence, the LODs of α-glucosidase / elastase could be estimated as the lowest concentration of α-glucosidase / elastase, for which I_F reaches the lowest detectable signal corresponding to a concentration of 0.1 µmol/L of the liberated 4-MU and 1.7 nmol/L of the liberated rhodamine 110 after different reaction times.

Detection of defined bacterial cultures.

One colony of *S. aureus* H560 (obtained from Ampli Phi Biosciences, UK)[39]; MSSA69[40],

eMRSA9[40] and MRSA378[40] (isolated from John Radcliffe Hospital, Headington, Oxford, OX3 9DU, UK) and *P. aeruginosa* PAO1/ATCC 15692 (purchased from Ampli Phi Bioscience, UK)[41,42,43] and PA887 (isolated from a chronic wound) were transferred from agar plates to a 15 mL reaction tubes with 5 mL LB medium and incubated at 37°C and 200 rpm for 18 hours. The bacterial suspensions used for MUD loaded NSC hydrogels were cultured under 150 rpm for 18 hours. Afterwards, the bacterial suspensions were diluted 1:100 in LB and incubated for a further 24 hours at 37°C. Finally, 100 µL of each bacterial suspension was added both elastase and α-glucosidase sensing hydrogels in 96-well plates and fluorescence intensity over time was measured (n = 3, technical triplicates). Each bacterial isolate was enumerated to determine viable bacterial cells by calculating the colony forming units per milliliter (CFU/mL), as outlined by Miles et al..[44] The detailed information about the relevant bacteria is provided in Table 1.

Table 1. The detailed information about the relevant bacteria.

Species	Strain	Source	Inoculum applied ($\times 10^9$ CFU/mL)		References
			in elastase sensing hydrogels	in α-glucosidase sensing hydrogels	
S. aureus	H560	obtained from Ampli Phi Biosciences, UK	5 (±1)	1.6 (± 0.1)	39
	MSSA69	isolated from John Radcliffe Hospital, Headington, Oxford, OX3 9DU, UK	2.2 (±0.8)	1.9 (± 0.5)	40
	eMRSA9		3 (± 2)	12.1 (± 0.8)	40
	MRSA378		4 (± 3)	0.6 (± 0.1)	40
P. aeruginosa	PAO1	ATCC 15692; purchased from Ampli Phi Bioscience, UK	4 (± 3)	4.7 (± 0.9)	41,42,43
	PA887	isolated from a chronic wound; acquired from Ampli Phi Biosciences, UK	7.7 (± 0.9)	3 (± 1)	

RESULTS AND DISCUSSION

In order to rapidly and selectively detect either *P. aeruginosa* or *S. aureus,* the enzyme-sensing hydrogel must detect characteristic bacterial enzymes for each of the species. This work focused on the detection of elastase for *P.* aeruginosa and α-glucosidase for *S. aureus*, as shown schematically in Figure 1.

The novel fluorescent probe (**ACS-HNE)** and the commercially available fluorescent probe MUD were loaded by entrapment into PVA and chitosan-based hydrogels, respectively. These hydrogels were subsequently shaped into the letters P and S, respectively, on a transparent plastic film using a PDMS mask. For *P. aeruginosa* detection, the elastase secreted by the bacteria cleaves peptide bonds in **ACS-HNE**, resulting in the fluorescence of rhodamine 110 in the P-shaped hydrogel. Conversely, most *S. aureus* strains express α-glucosidase[45], hence for *S. aureus* detection α-glucosidase cleaves the glyosidic bond in MUD, liberating the fluorescent 4-methylumbelliferone (4-MU) in the S-shaped hydrogel. Additionally, due to the distinct differences in emission wavelength of the two dyes, the liberated dyes can be differentiated under UV illumination using a hand-held lamp (λ_{ex} = 365 nm), which provides further distinction among the two bacterial species under investigation.
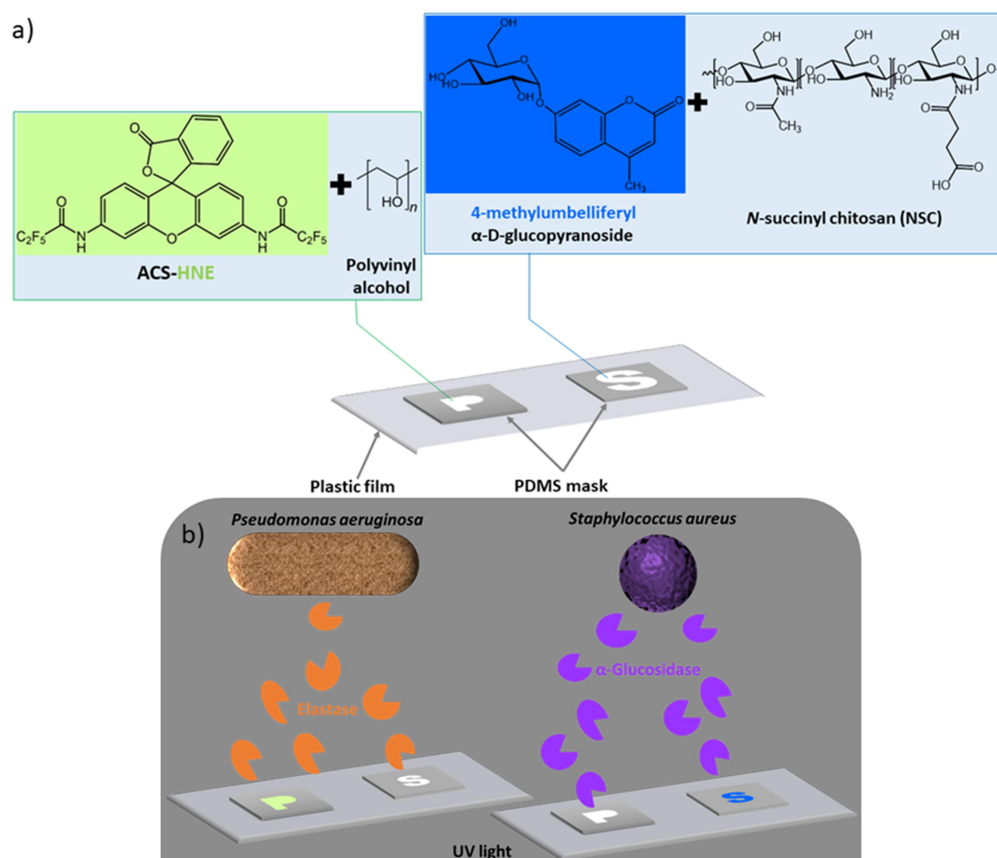
Figure 1. Schematics of the shape-encoded hydrogel sensors for detection and differentiation of *P. aeruginosa* and *S. aureus*. **a)** Chemical structures of fluorogenic substrates and hydrogel matrices. **b)** The fluorescence output in the form of the shape-encoded letters P (green) and S (blue) is defined by the corresponding target enzymes secreted from *P. aeruginosa* and *S. aureus*, respectively.

Hydrogel-based sensors and enzymatic reactions

The enzymatic reactions of the enzyme-sensing hydrogels were studied in neat buffered enzyme solutions (PBS, pH 7.4) and bacterial cultures of *P. aeruginosa* PAO1 and P887 or *S. aureus* MSSA69, MRSA378, eMRSA9 and H560 in LB medium. The fluorescent dyes RH110 (green) and 4-MU (blue) were formed during the corresponding enzymatic reaction. Fluorescence spectra of the enzymatic reaction occurring in enzyme-sensing hydrogels on silicon wafers were recorded in front-face illumination in a fluorescence spectrometer. Additionally, the apparent kinetics of the reaction was recorded using a microplate reader, in which the fluorescence intensity was measured in reflection from the top.
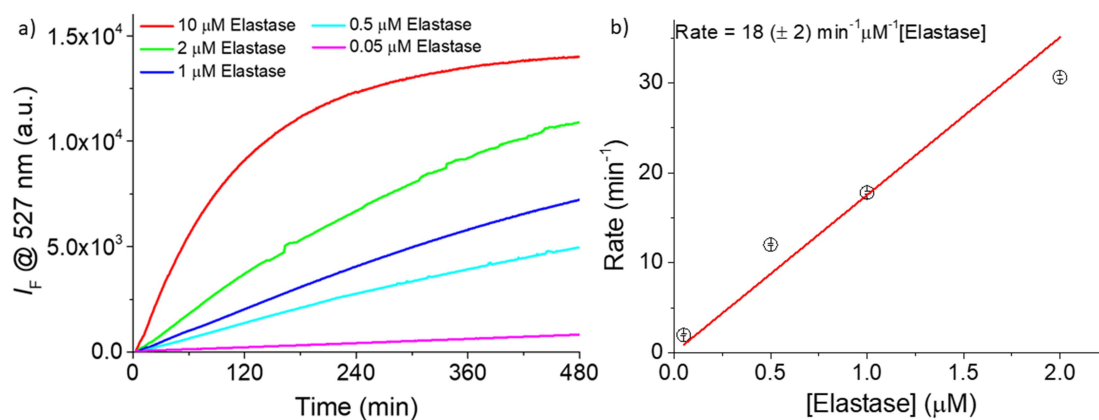
Enzymatic reaction of the elastase-sensing hydrogels. The enzymatic reaction of the elastase-sensing hydrogel on a silicon wafer was performed in neat buffered elastase solution (PBS, pH 7.4) and was recorded by fluorescence spectroscopy (Figure 2a). After the addition of elastase (150 µL, 10 µmol/L, PBS, pH 7.4), RH110 was liberated due to the enzymatic cleavage of the fluorescent probe **ACS-HNE** loaded into the PVA hydrogel. A monotonic increase of the fluorescence emission intensity (I_F) at $\lambda_{em} = 527$ nm was observed as a function of time (Figure 2b). The initial apparent rate in the first 30 min of the enzymatic reaction was found to be 0.79 min^{-1}.
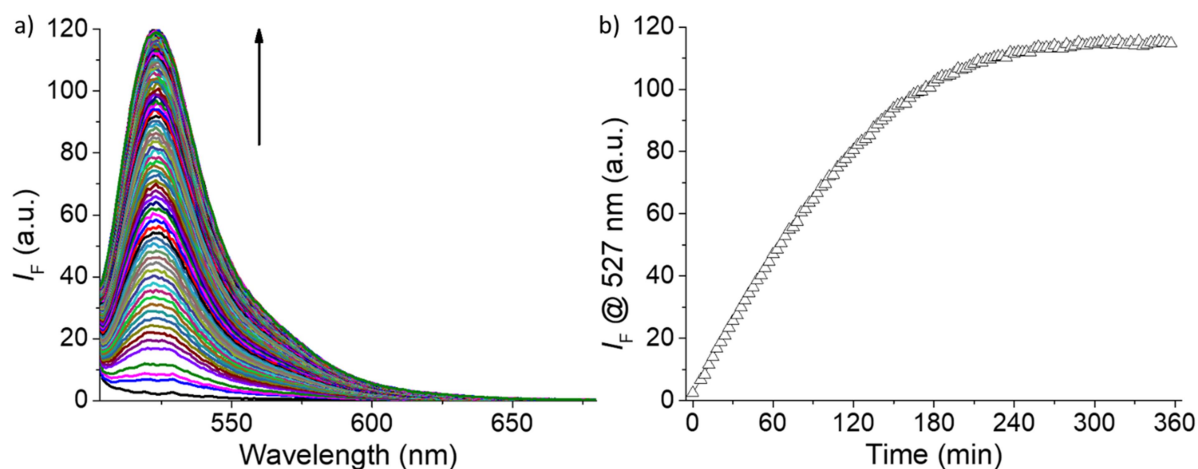
Figure 2. a) Fluorescence spectra (fluorescence spectrometer) of RH110 produced during the enzymatic reaction in the elastase-sensing PVA hydrogel on silicon ([**ACS-HNE**] = 5 μM; [Elastase] = 10 μM, PBS, pH 7.4, measurement repeat: 3 min, λ_{ex} = 496 nm, 25°C). b) Plot of fluorescence emission intensity at λ_{max} = 527 nm of RH110 in panel (a) versus time.
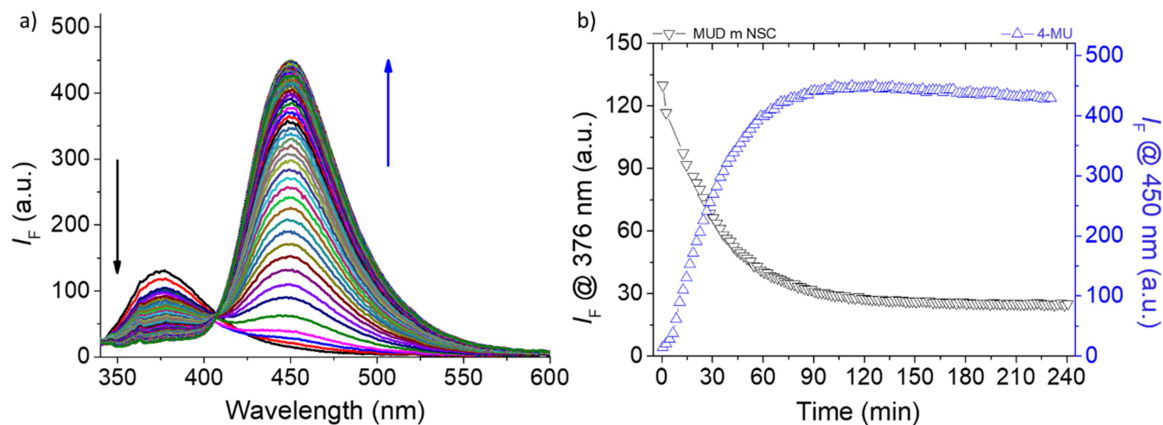
The kinetics of the enzymatic reaction in the hydrogel in a 96-well plate format with various concentration of elastase was recorded by sequential I_F measurements at λ_{max}. Plots of the I_F versus time are shown in Figure 3a. The initial apparent reaction rate (t ≤ 30 min) was found to depend linearly on the initial enzyme concentration. An apparent rate constant of 18 (± 2) $min^{-1}μM^{-1}$ was obtained (Figure 3b). Compared to the elastase-catalyzed reaction in **ACS-HNE** solution at the same substrate concentration,[34] the obtained initial apparent rate constant observed here is 3.3 times smaller, which is likely caused by slower diffusion of the enzyme into the hydrogel.[46] Although the use of the hydrogel slightly reduces the reaction rate, it helps to immobilize and handle / apply the fluorescent probe, which has limited water solubility.

Figure 3. Kinetics of the elastase-catalyzed cleavage of **ACS-HNE** that produces RH110 in the elastase-sensing PVA hydrogel. The fluorescence data obtained were used to calculate the LOD for the detection of the enzyme. a) I_F (λ_{max} = 527 nm) for RH110 formed in the reporter hydrogels incubated with various concentrations of enzyme solution versus time (blank-subtracted baseline: Kinetics of elastase-sensing PVA hydrogel in PBS solution. [**ACS-HNE**] = 5 µM, PBS solution (pH 7.4), measurement repeat: 1 min, λ_{ex} = 496 nm, 25°C). b) Plot of apparent reaction rate for the first 30 min from panel a) versus elastase concentration (R^2 = 0.9678, n = 3, the error bars show the standard deviation).

Additionally, to prove that the released RH110 was formed exclusively by enzymatic cleavage of the **ACS-HNE** inside the enzyme sensing hydrogel in the presence of elastase, the stability of the elastase-sensing hydrogel in neat PBS solution (pH 7.4) was tested as well as an enzymatic reaction using α-glucosidase, which is known not to catalyze the cleavage[34]. For these controls, the I_F at 527 nm increased by less than 7 % (relative to the same condition with 10 µM of elastase) after 6 hours (Figure S1a, S2a). Therefore, the elastase-sensing hydrogel can be utilized for the selective detection of elastase and differentiation from other enzymes, i.e. α-glucosidase.

Enzymatic reactions in α-glucosidase sensing hydrogels. The enzymatic reaction of the α-glucosidase-sensing hydrogel on silicon wafers was performed in neat buffered α-glucosidase solution (PBS, pH 7.4) and was recorded using a fluorescence spectrometer (Figure 4a). The change in the emission spectra after the addition of α-glucosidase (0.2 μM, in PBS) was caused by the conversion of the fluorescent probe MUD, loaded inside the NSC hydrogel, to the coumarin derivative 4-MU. The fluorescence emission peaks for MUD and 4-MU are located at about 375 nm and 450 nm, respectively, when excited at a wavelength λ_{ex} of 325 nm. A remarkably large increase in I_F at 450 nm and decrease in I_F at 375 nm was observed after the addition of α-glucosidase (0.2 μM, in PBS) over a period of 1.5 hours (Figure 4b). The initial apparent rate for the formation of 4-MU was found to be 9.3 min^{-1} in the first 30 min of the enzymatic reaction in the hydrogel.

Figure 4. a) Fluorescence spectra (fluorescence spectrometer) of 4-MU released during the enzymatic reaction inside the α-glucosidase-sensing NSC hydrogel on silicon ([MUD] = 1 mM; [α-Glucosidase] = 1.0 μM, PBS solution (pH 7.4), measurement repeat: 2 min, λ_{ex} = 325 nm, 25°C). b) Plot of fluorescence emission intensity at λ_{max} = 376 nm of MUD (initial) and at λ_{max} = 450 nm of 4-MU (product) in panel a) versus time.

The kinetics of the enzymatic reaction in the hydrogel in a 96-well plate format with various concentrations of elastase was recorded by sequential I_F measurements at $\lambda_{max.}$ The plots of I_F versus time are shown in Figure 5a. The initial apparent reaction rate (t ≤ 10 min) was found to depend linearly on the initial enzyme concentration and an apparent rate constant of 2.1×10^3 (± 0.1×10^3) min^{-1}µM^{-1} was obtained (Figure 5b). In order to prove that the formation of 4-MU is caused exclusively by catalysis of α-glucosidase, blank experiments were performed in PBS solution as well as in elastase solutions. A constant value of I_F at 450 nm was observed in the hydrogels, when exposed to PBS (Figure S1b) or elastase solution (Figure S2b). This indicates that the α-glucosidase-sensing hydrogel can be used for the detection and differentiation of α-glucosidase from elastase.
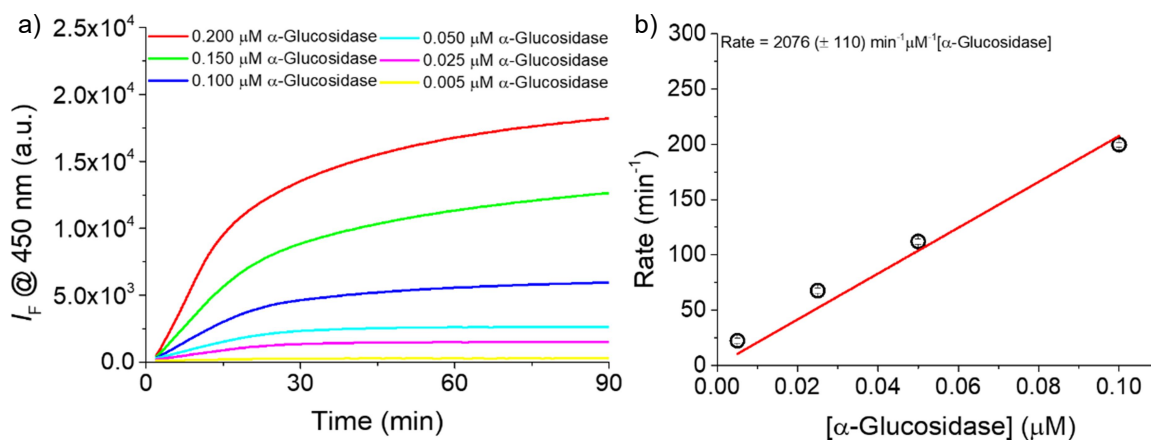
Figure 5. Kinetics of the α-glucosidase-catalyzed cleavage of MUD to 4-MU in the α-glucosidase-sensing NSC hydrogel. The fluorescence data obtained were used to calculate the LOD for the detection of the enzyme. a) I_F (λ_{max} = 450 nm) for 4-MU formed in the reporter hydrogels incubated with various concentrations of enzyme solution versus time (blank-subtracted baseline: Kinetics of α-glucosidase-sensing NSC hydrogel in PBS solution, [MUD] = 1 mM, PBS solution (pH 7.4), measurement repeat: 1 min, λ_{ex} = 365 nm, 25°C). b) Plot of

apparent reaction rates for the first 10 min from panel a) versus α-glucosidase concentrations (R^2 = 0.9887, n = 3, the error bars show the standard deviation).

Determination of the limit of detection

The limit of detection (LOD) for both enzymes is defined here as the lowest concentration of the corresponding enzyme that can be detected based on the release of the minimum detectable amount of reporter dye. The LOD for the detection of an enzyme can be estimated using the I_F values corresponding to the LOD for the detection of the dye divided by the value of the rate constant (calculated in Figures 4b) and 5b)) multiplied with the observation time. The corresponding plots of the LOD for elastase and α-glucosidase are shown in Figure 6 for a fixed loading of fluorescent probe in the hydrogels (0.3 µg / 100 µL of ACS-HNE loaded in elastase sensing hydrogel; 33.8 µg / 100 µL of MUD loaded in α-glucosidase sensing hydrogel). Consequently, the LODs of the enzyme sensing hydrogels for an observation time of 60 min using the microplate reader corresponded to enzyme concentrations of elastase and α-glucosidase of 17 nM and 0.2 nM, respectively. The elastase sensor here is slightly more sensitive than an enzyme substrate modified hydrogel sensor studied before (the LOD of elastase was reported to be 45 nM).[24] For α-glucosidase, this is an improvement of three orders of magnitude compared to the covalently attached fluorescent probe.[24]

Additionally, we found that the LOD for the detection of the enzyme was significantly improved by increasing the observation time and also by increasing the loading of the fluorescent probe in the hydrogel (see Figures S3 and S4 for comparison). Among our tested conditions, the best performance of the hydrogel sensor with the lowest LOD value of 27 pM for the detection of α-glucosidase at an observation time of 60 min was obtained by entrapping a maximum amount of

MUD into the NSC. The maximum loading was found to be 12 wt-%. Hence, we are able to maximize the sensitivity of the sensor hydrogel by maximizing the concentration of fluorescent probe in the hydrogel to reach the optimized detection condition.
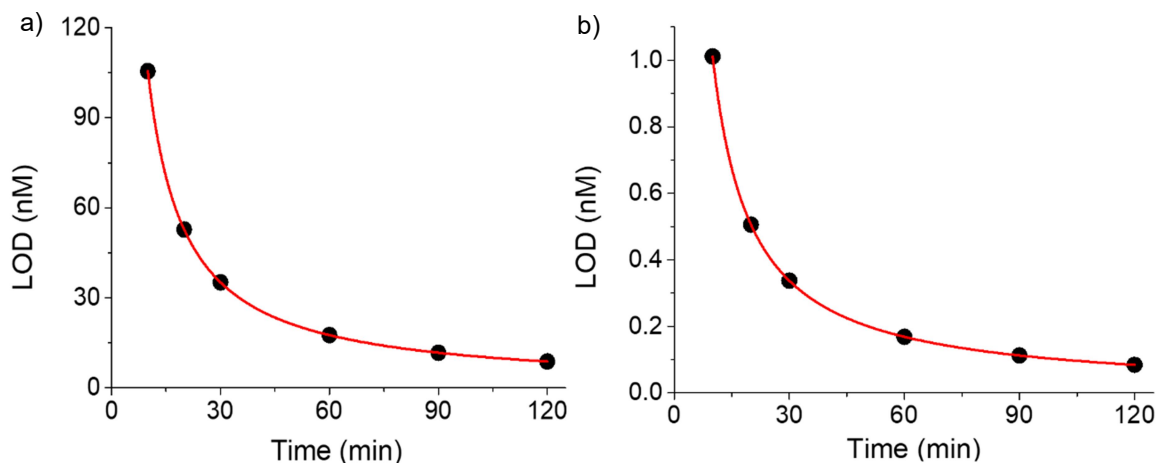
Figure 6. Plots of the LOD for a) elastase for the elastase-sensing PVA hydrogel, and for b) α-glucosidase for the α-glucosidase-sensing NSC hydrogel (microplate reader, 96 well plate, [**ACS-HNE**] = 5 µM, [**MUD**] = 1 mM, 25°C) The data were fitted with: a) $LOD_{(elastase)}$ = 1.1 µM min t^{-1}; b) $LOD_{(\alpha\text{-glucosidase})}$ = 10 nM min t^{-1}.

Enzyme-sensing hydrogels in bacterial suspensions.

As a further step to prove the functionality and selectivity of the enzyme-sensing hydrogels, they were tested using bacterial suspensions of *P. aeruginosa* and *S. aureus*. Bacterial detection using the enzyme-sensing hydrogel *in vitro* was performed by adding bacterial suspension (ca. 10^9 CFU/mL) into the wells of a 96 well plate containing the sensing hydrogels. Corresponding changes in fluorescence were recorded (Figure 7).

Bacteria-induced enzymatic reactions of elastase-sensing hydrogels. In Figure 7a, the monotonic increase of I_F at about 527 nm (λ_{ex} of 496 nm) is associated with the formation of RH110 as a function of time in the presence of different *P. aeruginosa* (PAO1 and P887) and *S. aureus* (MSSA69, MRSA378, eMRSA9 and H560) suspensions. The slope (for $t < 1$ hour) for *P. aeruginosa* suspensions was found to be more than two times larger than that for suspensions of *S. aureus*. This finding is fully consistent with a substantial secretion of elastase by *P. aeruginosa*.[47] The increase in signal observed for *S. aureus* cultures is attributed to the limited longtime stability of the **ACS-HNE** probe, which results in the hydrolysis of the **ACS-HNE** substrate in the hydrogel after the addition of *S. aureus*, similar to the blank results obtained in LB medium (Figure S5a). Here an increase of the I_F signal at 527 nm was observed, as is shown in Figure S5a, indicating that some RH110 was cleaved from **ACS-HNE**, in the absence of elastase. In addition, we cannot exclude that the increase of the I_F signal in case of *S. aureus* might also be caused by secretion products of *S. aureus* other than elastase.

Bacteria induced enzymatic reactions of α-glucosidase-sensing hydrogels. In Figure 7b, a monotonic increase of I_F at 460 nm at 25°C was observed as a function of time during the enzymatic reaction of α-glucosidase-sensing hydrogels in suspensions of four different *S. aureus* strains (MSSA69, MRSA378, eMRSA9 and H560). The increase observed in all cases is associated to the formation of liberated deprotonated 4-MU. The varying slopes (< 6 hours) show different kinetics among the reaction in different *S. aureus* suspensions, which is likely caused caused by different amounts of α-glucosidase produced and secreted during bacterial growth. This could be attributed to (*i*) different growth characteristics of different bacterial strains and (*ii*) different expression of genes in culture.[48] On the contrary, the value of I_F kept constant after the addition of suspensions of two different *P. aeruginosa* strains (PAO1 and P887), as well as in the

control (LB medium, Figure S5b). Hence, the α-glucosidase-sensing hydrogel was shown to detect the bacteria and to differentiate *S. aureus* from *P. aeruginosa* strains among a broad range of different strains.

The combined results confirm that the enzyme-sensing hydrogels reported here can not only be used for the rapid, sensitive and selective bacterial enzyme detection and differentiation, but can also be used to differentiate planktonic suspensions of *P. aeruginosa* from *S. aureus*.
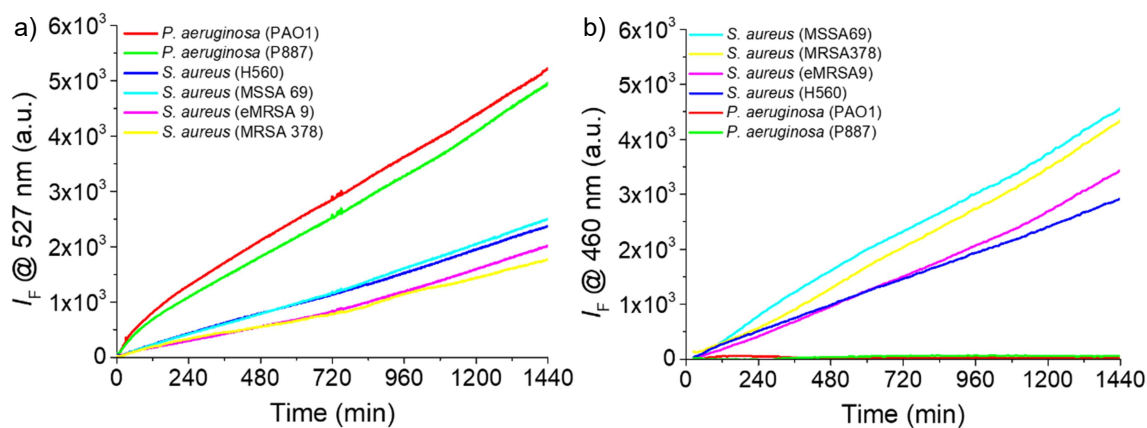
Figure 7. *In situ* measurement of enzyme-sensing hydrogels in bacterial suspensions using a microplate reader. I_F of a) RH110 released from the elastase-sensing hydrogel at $\lambda_{max} = 527$ nm and b) 4-MU released from the α-glucosidase-sensing hydrogel at $\lambda_{ex} = 460$ nm versus time during the enzymatic reaction of the hydrogels with suspensions of different *P. aeruginosa* and *S. aureus* strains (subtracted baseline: Kinetics of enzyme sensing hydrogel in LB medium; Measurement repeat: 1 min, 25°C, for a) [**ACS-HNE**] = 5 µM, $\lambda_{ex} = 496$ nm, for b) [MUD] = 1 mM, $\lambda_{ex} = 365$ nm).

Enzymatic Reactions in Patterned Enzyme Sensing Hydrogels.

Finally, patterned enzyme sensing hydrogels were applied for the rapid detection and discrimination of elastase and α-glucosidase. The photograph shown in Figure 8 was taken by a

mobile phone camera 1 hour after the addition of the enzyme solution(s). The illumination was afforded by a standard hand-held UV lamp (λ_{ex} = 365 nm).

After 60 min, significant fluorescence was visible under UV illumination only in the P-shaped pattern in the 2nd and 3rd rows in the left column of the elastase-sensing hydrogel (green), attributed to the released RH110. Similarly, the blue fluorescence of 4-MU was visible exclusively in the 1st and 3rd rows in the right column, where the α-glucosidase-sensing hydrogel was exposed to the enzyme solution that contained α-glucosidase. No fluorescence signal was observed in the last row, where only PBS solution was added to the enzyme sensing hydrogel as a negative control.

In addition, it was confirmed by independent spectroscopic measurements that the off-target enzymes could not break the labile bond in the fluorescent probes and therefore did not result in any bare eye visible signal under illumination at 365 nm, as shown in Figure 8 (left pattern in the 1st row, and right pattern in the 2nd row). Hence, the shape encoded enzyme sensing hydrogels afforded a simple and double redundant readout for the bacterial enzyme detection and differentiation by bare eye.

Figure 8. Photograph of the shape-encoded enzyme sensing hydrogels after enzymatic reactions. The photo was taken after a reaction time of 60 min under UV illumination (hand-held lamp, λ_{ex} = 365 nm) on a black background ([MUD] = 1 mM, **[ACS-HNE]** = 5 µM, individual enzyme solutions [α-Glucosidase] = 1.0 µM, [Elastase] = 10 µM were added in the 1st and 2nd row, respectively. A mixed enzyme solution ([α-Glucosidase] = 2.0 µM, [Elastase] = 20 µM with a volume ratio of 1:1) was applied in each letter patterns at the 3rd row. PBS was added in the

bottom row. The length and thickness of the square PDMS mask are about 1.9 cm and 2.8 mm, 80 µL of the enzyme solution was applied into each letter area.

The unique shape and color under UV illumination, corresponding to the characteristic bacterial enzyme, is the central asset of the demonstrated strategy for the rapid identification of specific bacterial species, showcasing the potential utility of this product as an effective point of care test that could be simply read by non-specialists. Overall, the sensors developed in this work show excellent performance in bacterial enzyme detection and discrimination, by simply entrapping fluorescent probes into the hydrogel. Firstly, the sensor hydrogels show extremely low LOD values for their target enzyme. When using the same amount of fluorescent probe, the LOD for α-glucosidase (27 pM) detected by the hydrogel in this work, is much lower than that in the literature (20 nM)[24], and also a very recently improved covalent variant (200 pM)[38], in which MUD was covalently grafted to the hydrogel. The values of the LOD (for the same observation time) are improved by increasing the loading with the probe and thereby increasing the rate of the enzymatic reaction according to Michaelis-Menten kinetics in both cases.[49] Unlike the chemical modification method that was used in studies before, which is inherently limited by the corresponding grafting efficiency, the physical entrapment allows one to increase the concentration of the fluorescent probe inside the hydrogels. In Figure S6, the apparent rate constant is shown to increase with higher loading of MUD in the α-glucosidase-sensing NSC hydrogels. Using the same loading for chemical attachment and physical entrapment of MUD (at about 33.8 µg, 100 µL), the grafting efficiency is estimated to be approx. 44% by comparing the corresponding spectra of this current study with those in the previous work[38]), the apparent rate constant obtained by the physical entrapment technique ($\sim 2.7 \times 10^3$ min^{-1}µM^{-1}, estimated

according to the function in Figure S6) is larger than the one observed with grafted probes (~ 1.8 $\times$ 10^3 min^{-1}µM^{-1}).[38] This is likely due to reduced availability of grafted substrates compared to the entrapped fluorescent probe in the hydrogel. Larger apparent rate constants consequently result in an improved LOD. Hence, the lower LOD observed here is attributed to increased loading and thus higher concentration of fluorescent probes in the hydrogel on the one hand, and to enhanced availability of physically entrapped fluorescent probes on the other hand. While chemical grafting affords a better fixation of fluorescent probes in the hydrogel, and may thus be beneficial in long term storage or sterilization, covalent attachment of the probes to the polymers limits the attainable loading and may reduce the accessibility and reactivity in the enzymatic reaction. Additionally, using the physical entrapment technique explored in this work, the loading of the substrate could be easily varied. This was shown by encapsulating a novel fluorophore **ACS-HNE**, previously developed by members of this team,[34] into a PVA hydrogel, resulting in the selective detection of *P. aeruginosa* cultures via the detection of elastase.

CONCLUSION

Shape-encoded hydrogel sensors with physically entrapped fluorescent probes were utilized successfully to sensitively and selectively detect and discriminate elastase and α-glucosidase, which are secreted by *P. aeruginosa* and *S. aureus*, respectively. The elastase-sensing hydrogels, which contained the novel fluorogenic elastase substrate **ACS-HNE,** were shown to detect elastase within 60 min using a conventional microplate reader with an improved LOD of 20 nM. Compared to previous reports, an LOD of <30 pM for the α-glucosidase-sensing MUD equipped hydrogel, constitutes an improvement of three orders of magnitude compared to previously published results for chitosan-based sensor hydrogels. This improvement of the LOD was

achieved by increasing the amount of loaded fluorescent probe in the hydrogel. *In vitro* tests with bacterial suspensions demonstrated the ability of these hydrogels to detect and differentiate among defined *P. aeruginosa* and *S. aureus* cultures. The shape and color encoded strategy shows potential for the future development of an effective and simple point-of-care test for the rapid identification of bacterial species, which can be used by non-specialists.

ASSOCIATED CONTENT

Supporting Information. Kinetics data for blank experiments in PBS and LB medium, negative enzyme controls, data for determination of the LOD, as well as effects of observation time and fluorescent probe loading in the hydrogel on the LOD of enzyme. (PDF)

AUTHOR INFORMATION

Corresponding Author

*E-mail: schoenherr@chemie.uni-siegen.de

Author Contributions

The manuscript was written through contributions of all authors. All authors have given approval to the final version of the manuscript.

ABBREVIATIONS

ACS-HNE:	N,N'-(3-oxo-3H-spiro[isobenzofuran-1,9'-xanthene]-3',6'-diyl)bis(2,2,3,3,3 pentafluoropropanamide)
DMSO:	Dimethyl sulfoxide
LB medium:	Luria-Bertani medium
LOD:	Limit of detection
MDR:	Multi-drug Resistant
MRSA:	Methicillin-resistant *Staphylococcus aureus*
4-MU:	4-Methylumbelliferone
MUD:	4-Methylumbelliferyl α-D-glucopyranoside
NSC:	*N*-succinyl-chitosan

P. aeruginosa: *Pseudomonas aeruginosa*

PBS: Phosphate-buffered saline

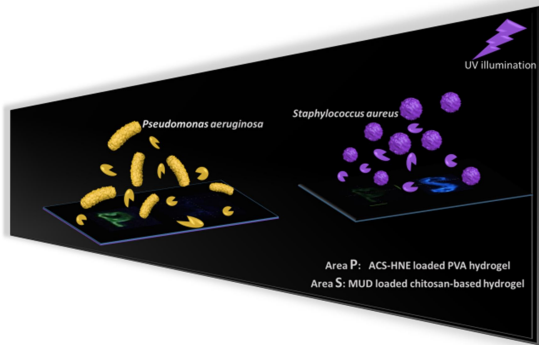PCR: Polymerase chain reaction

PDMS: Polydimethylsiloxane

PVA: Polyvinyl alcohol

RH110:   Rhodamine 110

S. aureus: *Staphylococcus aureus*

ToC Graphic

REFERENCES

[1] Horcajada, J. P.; Montero, M.; Oliver, A.; Sorlí, L.; Luque, S.; Gómez-Zorrilla, S.; Benito, N.; Grau, S. Epidemiology and Treatment of Multidrug-Resistant and Extensively Drug-Resistant *Pseudomonas aeruginosa* Infections. *Clin. Microbiol. Rev.* **2019**, *32*, e00031-19.

[2] CDC. *Antibiotic Resistance Threats in the United States*, **2019**. Atlanta, GA: U.S. Department of Health and Human Services, CDC; 2019. https://www.cdc.gov/DrugResistance/Biggest-Threats.html.

[3] Ventola, C. L. The Antibiotic Resistance Crisis: Part 1: Causes and Threats. *Pharm. Ther.* **2015***, 40,* 277–283.

[4] Tong, S. Y. C.; Davis, J. S.; Eichenberger, E.; Holland, T. L.; Fowler, V. G. *Staphylococcus aureus* Infections: Epidemiology, Pathophysiology, Clinical Manifestations, and Management. *Clin. Microbiol. Rev.* **2015**, *28*, 603-661.

[5] Wu, S.; Duan, N.; Gu, H.; Hao, L.; Ye, H.; Gong, W.; Wang, Z. A Review of the Methods for Detection of *Staphylococcus aureus* Enterotoxins. *Toxins* **2016**, *8*,176.

[6] Fooladvand, S.; Sarmadian, H.; Habibi, D.; van Belkum, A.; Ghaznavi-Rad, E. High Prevalence of Methicillin Resistant and Enterotoxin Gene-Positive *Staphylococcus aureus* Among Nasally Colonized Food Handlers in Central Iran. *Eur. J. Clin. Microbiol. Infect. Dis.* **2019**, *38*, 87-92.

[7] Magill, S. S.; Edwards, J. R.; Bamberg, W.; Beldavs, Z. G.; Dumyati, G.; Kainer, M. A.; Lynfield, R.; Maloney, M.; McAllister-Hollod, L.; Nadle, J.; Ray, S. M.; Thompson, D. L.; Wilson, L. E.; Fridkin, S. K.; and Emerging Infections Program Healthcare-Associated Infections and Antimicrobial Use Prevalence Survey Team (2014) Multistate Point-Prevalence Survey of Health Care-Associated Infections. *N. Engl. J. Med.* **2014**, *370*, 1198-1208.

[8] *Members in Centers for Disease Control and Prevention.* Deadly Staph Infections Still Threaten the U.S.: CDC Calls for Increased Prevention to Protect Patients (accessed November 5, 2019). https://www.cdc.gov/media/releases/2019/p0305-deadly-staph-infections.html

[9] Váradi, L.; Luo, J. L.; Hibbs, D. E.; Perry, J. D.; Anderson, R. J.; Orenga, S.; Groundwater, P. W. Methods for the Detection and Identification of Pathogenic Bacteria: Past, Present, and Future. *Chem. Soc. Rev.* **2017**, *46*, 4818-4832.

[10] Rajapaksha, P.; Elbourne, A.; Gangadoo, S.; Brown, R.; Cozzolino, D.; Chapman, J. A Review of Methods for the Detection of Pathogenic Microorganisms. *The Analyst* **2019**, *144*, 396-411.

[11] Lazcka, O.; Del Campo, F. J.; Muñoz, F. X. Pathogen Detection: a Perspective of Traditional Methods and Biosensors. *Biosens. Bioelectron.* **2007**, *22*, 1205-1217.

[12] Caliendo, A. M.; Gilbert, D. N.; Ginocchio, C. C.; Hanson, K. E.; May, L.; Quinn, T. C.; Tenover, F. C.; Alland, D.; Blaschke, A. J.; Bonomo, R. A.; Carroll, K. C.; Ferraro, M. J.; Hirschhorn, L. R.; Joseph, W. P.; Karchmer, T.; MacIntyre, A. T.; Reller, L. B.; Jackson, A. F.; and Infectious Diseases Society of America (IDSA) (2013) Better Tests, Better Care: Improved Diagnostics for Infectious Diseases. *Clin. Infect. Dis.* **2013**, *57*, S139-70.

[13] Hameed, S.; Xie, L.; Ying, Y. Conventional and Emerging Detection Techniques for Pathogenic Bacteria in Food Science: A Review. *Trends Food Sci. Technol.* **2018**, *81*, 61-73.

[14] Singh, R.; Mukherjee, M. D.; Sumana, G.; Gupta, R. K.; Sood, S.; Malhotra, B. D. Biosensors for Pathogen Detection: A Smart Approach Towards Clinical Diagnosis. *Sens. Actuators, B* **2014**, *197*, 385-404.

[15] Fach, P.; Perelle, S.; Dilasser, F.; Grout, J.; Dargaignaratz, C.; Botella, L.; Gourreau, J.-M.; Carlin, F.; Popoff, M. R.; Broussolle, V. Detection by PCR-Enzyme-Linked Immunosorbent

Assay of Clostridium Botulinum in Fish and Environmental Samples from a Coastal Area in Northern France. *Appl. Environ. Microbiol.* **2002**, *68*, 5870-5876.

[16] Miñán, A.; Bosch, A.; Lasch, P.; Stämmler, M.; Serra, D. O.; Degrossi, J.; Gatti, B.; Vay, C.; D'aquino, M.; Yantorno, O.*;* Naumann, D. Rapid Identification of *Burkholderia cepacia* Complex Species Including Strains of the Novel Taxon K, Recovered from Cystic Fibrosis Patients by Intact Cell MALDI-ToF Mass Spectrometry. *The Analyst* **2009**, *134*, 1138-1148.

[17] Li, H.; Zhu, J. Differentiating Antibiotic-Resistant *Staphylococcus aureus* Using Secondary Electrospray Ionization Tandem Mass Spectrometry. *Anal. Chem.* **2018**, *90*, 12108-12115.

[18] Lukumbuzya, M.; Schmid, M.; Pjevac, P.; Daims, H. A Multicolor Fluorescence *in situ* Hybridization Approach Using an Extended Set of Fluorophores to Visualize Microorganisms. *Front. Microbiol.* **2019**, *10*, 1383.

[19] Suaifan, G. A. R. Y.; Alhogail, S.; Zourob, M. Rapid and Low-Cost Biosensor for the Detection of *Staphylococcus aureus*. *Biosens. Bioelectron.* **2017**, *90*, 230-237.

[20] Chen, Y.; Cheng, N.; Xu, Y.; Huang, K.; Luo, Y.; Xu, W. Point-of-Care and Visual Detection of *P. aeruginosa* and its Toxin Genes by Multiple LAMP and Lateral Flow Nucleic Acid Biosensor. *Biosens. Bioelectron.* **2016**, *81*, 317-323.

[21] Zhou, J.; Hou, S.; Li, L.; Yao, D.; Liu, Y.; Jenkins, A. T. A.; Fan, Y. Theranostic Infection-Responsive Coating to *in situ* Detect and Prevent Urinary Catheter Blockage. *Adv. Mater. Interfaces* **2018**, *5*, 1801242.

[22] Mostafalu, P.; Tamayol, A.; Rahimi, R.; Ochoa, M.; Khalilpour, A.; Kiaee, G.; Yazdi, I. K.; Bagherifard, S.; Dokmeci, M. R.; Ziaie, B.; Sonkusale, S. R.; Khademhosseini, A. Smart Bandage for Monitoring and Treatment of Chronic Wounds. *Small* **2018**, *14*, 1703509.

[23] Mirani, B.; Pagan, E.; Currie, B.; Siddiqui, M. A.; Hosseinzadeh, R.; Mostafalu, P.; Zhang, Y. S.; Ghahary, A.; Akbari, M. An Advanced Multifunctional Hydrogel-Based Dressing for Wound Monitoring and Drug Delivery. *Adv. Healthcare Mater.* **2017**, *6*, 1700718.

[24] Ebrahimi, M.-M. S.; Laabei, M.; Jenkins, A. T. A.; Schönherr, H. Autonomously Sensing Hydrogels for the Rapid and Selective Detection of Pathogenic Bacteria. *Macromol. Rapid Commun.* **2015**, *36*, 2123-2128.

[25] Azghani, A. O.; Bedinghaus, T.; Klein, R. Detection of Elastase from *Pseudomonas aeruginosa* in Sputum and its Potential Role in Epithelial Cell Permeability. *Lung* **2000**, *178*, 181-189.

[26] Pelletier, A.; Dimicoli, J. L.; Boudier, C.; Bieth, J. G. Nonchromogenic Hydrolysis of Elastase and Cathepsin G p-Nitroanilide Substrates by *Pseudomonas aeruginosa* Elastase. *Am. J. Respir. Cell Mol. Biol.* **1989**, *1*, 37-39.

[27] Goldberg, J. B.; Ohman, D. E. Activation of an Elastase Precursor by the lasA Gene Product of *Pseudomonas aeruginosa*. *J. Bacteriol.* **1987**, *169*, 4532-4539.

[28] Kim, J. Y.; Sahu, S; Yau, Y. H.; Wang, X.; Shochat, S. G.; Nielsen, P. H.; Dueholm, M. S.; Otzen, D. E.; Lee, J.; Santos, M. M. S. D.; Yam, J. K. H.; Kang, N. Y.; Park, S. J.; Kwon, H.; Seviour, T.; Yang, L.; Givskov, M.; Chang, Y. T. Detection of Pathogenic Biofilms with Bacterial Amyloid Targeting Fluorescent Probe, CDy11. *J. Am. Chem. Soc.* **2016**, *138*, 402-407.

[29] Yoon, J. W.; Kim, S.; Yoon, Y.; Lee, M. H. A Resorufin-based Fluorescent Turn-on Probe Responsive to Nitroreductase Activity and its Application to Bacterial Detection. *Dyes Pigm.* **2019**, *171*, 107779.

[30] Wang, W.; Wang, Y.; Lin, L.; Song, Y.; Yang, C. J. A Tridecaptin-based Fluorescent Probe for Differential Staining of Gram-negative Bacteria. *Anal. Bioanal.Chem.* **2019**, *411*, 4017-4023.

[31] Xu, S.; Wang, Q.; Zhang, Q.; Zhang, L.; Zuo, L.; Jiang, J. D.; Hu, H. Y. Real Time Detection of ESKAPE Pathogens by a Nitroreductase-Triggered Fluorescence Turn-on Probe. *Chem. Commun.* **2017**, *53*, 11177-11180.

[32] Kwon, H. Y.; Liu, X.; Choi, E. G.; Lee, J. Y.; Choi, S. Y.; Kim, J. Y.; Wang, L.; Park, S. J.; Kim, B.; Lee, Y. A.; Kim, J. J.; Kang, N. Y.; Chang, Y. T. Development of Universal Fluorescent Gram-positive Bacteria Probe. *Angew. Chem. Int. Ed.* **2019**, *58*, 8426.

[33] Kang, E. B.; Mazrad, Z. A. I.; Robby, A. I.; In, I.; Park, S. Y. Alkaline Phosphatase-Responsive Fluorescent Polymer Probe Coated Surface for Colorimetric Bacteria Detection. *Eur. Polym. J.* **2018**, *105*, 217-225.

[34] Jia, Z.; Han, H. H.; Sedgwick, A. C.; Williams, G. T.; Gwynne, L.; Bull, S.D.; Jenkins, A. T. A.; He, X. P.; Schönherr, H.; Sessler, J. L.; James, T. D. Protein Encapsulation: A Nanocarrier Approach to the Fluorescence Imaging of an Enzyme-based Biomarker. *Front. Chem.* **2020**, *8*, article 389.

[35] Mukhopadhyay P.; Sarkar, K.; Bhattacharya, S.; Bhattacharyya, A.; Mishra, R.; Kundu, P. P. pH Sensitive *N*-succinyl Chitosan Grafted Polyacrylamide Hydrogel for Oral Insulin Delivery. *Carbohydr. Polym.* **2014**, *112*, 627–637.

[36] Yan, C.; Chen, D.; Gu, J.; Hu, H.; Zhao, X.; Qiao, M. Preparation of N-succinyl-chitosan and its Physical-chemical Properties as a Novel Excipient, *J. Pharm. Soc. Jpn.* **2006**, *126*,789–793.

[37] Kumar, A.; Whitesides, G. M. Features of Gold Having Micrometer to Centimeter Dimensions can be Formed Through a Combination of Stamping with an Elastomeric Stamp and an Alkanethiol ''Ink'' Followed by Chemical Etching. *Appl. Phys. Lett.* **1993**, *63*, 2002-2004.

[38] Jia, Z.; Müller, M.; Le Gall, T.; Riool, M.; Müller, M.; Zaat, S. A. J.; Montier, T.; Schönherr, H. Multiplexed Bacterial Enzyme Differentiation and Bacteria Detection by Color-encoded Sensor Hydrogels, *Biomaterials* **2020***, to be submitted***.**

[39] Esteban, P. P.; Jenkins, A. T. A.; Arnot, T. C. Elucidation of the Mechanisms of Action of Bacteriophage K / Nano-emulsion Formulations Against *S. aureus* via Measurement of Particle Size and Zeta Potential. *Colloids Surf.* **2016**, *130*, 87-94.

[40] Peacock, S. J.; Moore, C. E.; Justice, A.; Kantzanou, M.; Story, L.; Mackie, K.; O'Neill, G.; Day, N. P. J. Virulent Combinations of Adhesin and Toxin Genes in Natural Populations of *Staphylococcus aureus*. *Infect. Immun.* **2002**, *70*, 4987–4996.

[41] Holloway, B. W. Genetic Recombination in *Pseudomonas aeruginosa. J. Gen. Microbiol.* **1955**, *13*, 572-581.

[42] Cox, C. D. Effect of Pyochelin on the Virulence of *Pseudomonas aeruginosa. Infect Immun.* **1982,** *36*, 17–23.

[43] Stover, C. K.; Pham, X. Q.; Erwin, A. L.; Mizoguchi, S. D.; Warrener, P.; Hickey, M. J.; Brinkman, F.S. L.; Hufnagle, W. O.; Kowalik, D. J.; Lagrou, M.; Garber, R. L.; Goltry, L.; Tolentino, E.; Westbrock-Wadman, S.; Yuan, Y.; Brody, L. L.; Coulter, S. N.; Folger, K. R.; Kas, A.; Larbig, K.; Lim, R.; Smith, K.; Spencer, D.; Wong, G. K.-S.; Wu, Z.; Paulsen, I. T.; Reizer, J.; Saier, M. H.; Hancock, R. E. W.; Lory, S.; Olson, M. V. Complete Genome Sequence of *Pseudomonas aeruginosa* PAO1, an Opportunistic Pathogen. *Nature,* **2000**, *406*, 959–964.

[44] Miles, A. A.; Misra, S. S.; and Irwin, J. O. The Estimation of the Bactericidal Power of the Blood. *J. Hyg. (London)* **1938**, *38*, 732–49.

[45] Fontana, C.; Laratta, E.; Marino, D.; Pistoia, E. S.; Favalli, C. Simple Enzymatic Method for Rapid Identification of a *Staphylococcus aureus* Subspeciesaureus Biovar. *Eur. J. Clin. Microbiol. Infect. Dis.* **1997**, *16*, 689–692.

[46] Lieleg, O.; Ribbeck, K. Biological Hydrogels as Selective Diffusion Barriers. *Trends Cell Biol.* **2011**, *21*, 543–551.

[47] Kamath S.; Kapatral, V.; Chakrabarty, A. M; Cellular Function of Elastase in *Pseudomonas aeruginosa*: Role in the Cleavage of Nucleoside Diphosphate Kinase and in Alginate Synthesis. *Mol. Microbiol.* **1998**, *30*, 933-941.

[48] Liu, L.; Yang, H.; Shin, H.-d.; Chen, R. R.; Li, J.; Du, G.; Chen, J. How to Achieve High-level Expression of Microbial Enzymes: Strategies and Perspectives. *Bioengineered* **2013**, *4*, 212–223.

[49] Nelson, D., and Cox, M. Lehninger: Principles of Biochemistry (4th ed.), W.H. Freeman and Company, **2005**, New York. ISBN: 0-7167-4339-6.